MODELING GROUNDWATER – SEAWATER INTERACTIONS IN THE ARAL SEA REGION

Y. SHIBUO✉, J. JARSJÖ, and G. DESTOUNI

Department of Physical Geography and Quaternary Geology, Stockholm University, SE-106 91 Stockholm, Sweden
E-mail:yoshihiro.shibuo@natgeo.su.se
E-mail:jerker.jarsjo@natgeo.su.se
E-mail:georgia.destouni@natgeo.su.se

Abstract

Changes due to failed mega-hydrological engineering following the 1960's have led to dramatic shrinkage and salinisation of the Aral Sea. We consider a characteristic cross-section of the south-eastern coastal region of the Large Aral Sea in the vicinity of the Amu Darya river delta, and investigate through numerical simulation, the changing of submarine groundwater discharge (SGD) and saltwater intrusion into the coastal aquifer, under observed changes in regional hydrologic conditions during 1960-1964, e.g., resulting in a seaward shoreline movement of 2.8 kilometres. The results indicate that the net SGD into the Aral Sea exhibited an overall decrease over the simulation period, although there is a trend of increase following the relatively large initial decrease. The seaward fresh groundwater discharge exhibits a small yet systematic increase over the simulation period, during which seawater density did not change much and the mean groundwater hydraulic gradient could not change much, due to the generally flat topography and bathymetry of the south-eastern Aral Sea coast. Groundwater in the vicinity of the original, pre-1960 shoreline remained brackish, with salinity around 10g/L, indicating a remaining aquifer vulnerability to seawater intrusion.

Keywords: Aral Sea; Salinisation; Seawater – Freshwater interaction; Hydrostatic pressure balance

Introduction

Submarine groundwater discharge (SGD) from coastal aquifers into the sea may be considerable, possibly even in comparison with stream and river discharges (Moore, 1996). At the same time, coastal aquifers and their freshwater resources are generally vulnerable to intrusion of the heavier seawater, with many cases of such seawater intrusion being reported in coastal areas and islands all over the world (e.g., Koussis *et al.*, 2002).

✉ Corresponding author

The Aral Sea, being a brackish water lake with salinity of approximately 10g/L before the 1960's, has since then experienced dramatic shrinkage and salinisation due to failed mega-hydrological engineering project (Figure 1). The Aral Sea volume currently constitutes less than one tenth of the original, pre-1960 volume (Kostianoy *et al.*, 2004). Furthermore, in 1989 the Aral Sea split into two separate water bodies, known as Small Aral (in the north, with the Syr Darya river as the single principal source of surface water inflow) and Large Aral (in the south, with the Amu Darya river as the single principal source of surface water inflow). As a result of this shrinking process, salts enrich in remaining water volumes. By 1992, the salinity reached the mean ocean salinity of 35 g/L in Large Aral. Whereas the salinity of Small Aral remains below ocean salinity (Aladin *et al.*, 2004), the salinity of Large Aral increased considerably during the 1990's and is now (2003) as high as 90 g/L (Zavialov *et al.*, 2003). In addition, the Amu Darya river water is saline; in the Aral Sea vicinity (at the Kiziljar monitoring station) monthly averages of river salinity ranges between 0.7 and 3 g/L, and a considerable stretch of Amu Darya has higher salinity than the Uzbek freshwater quality standard of 1g/L for most part of the year (Froebrich and Kayumov, 2004). In this region, groundwater constitutes the only remaining freshwater source that can meet this water quality standard.

Recently, Jarsjö and Destouni (2004) investigated the fresh groundwater inflow to the shrinking Aral Sea, showing that its relative importance has increased dramatically, from constituting about 12% of total river discharge in 1960, to about 100% of the drastically reduced discharges of the Amu Darya and Syr Darya rivers in recent years. In addition, the results of Jarsjö and Destouni (2004) indicated a regional variability

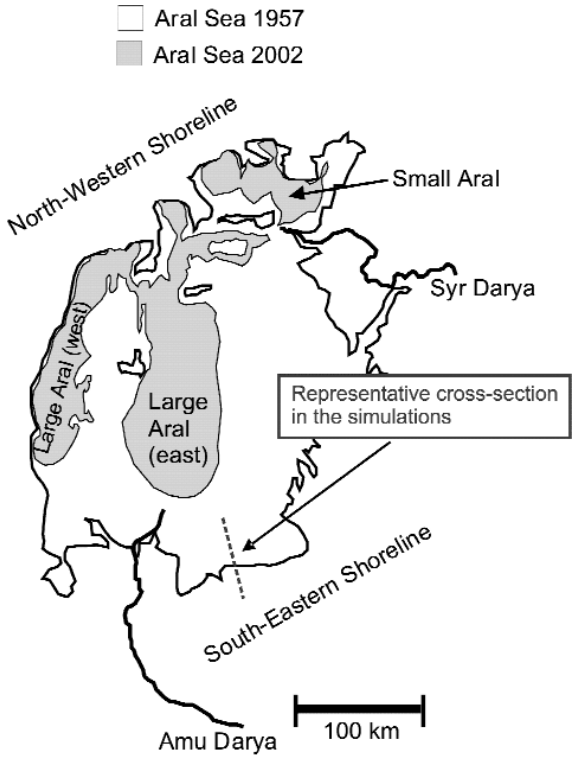

Figure 1. Location of the representative simulated aquifer cross-section in the South-Eastern Aral Sea region.

of changes in fresh groundwater discharge into the Aral Sea since 1960, with essentially unchanged discharge in the Amu Darya delta region, and considerable groundwater discharge increases in other regions around the Large Aral Sea.

In this study, we particularly address the groundwater-seawater interactions that result from density-driven subsurface flows in the water-stressed coastal region of Large Aral Sea in the Amu Darya delta vicinity. One main goal is to investigate the potential for saltwater intrusion into the coastal aquifer and its freshwater resources, given the exceptional previous and still on-going changes in regional hydrologic conditions. On the one hand, the Aral Sea level lowering, in itself, implies decreased salt water intrusion risk and, on the other hand, increasing salt content and density of the seawater should imply an increased potential for density-driven seawater intrusion. In the following, we investigate the combined effect of such changing boundary conditions on the subsurface flows in the groundwater-coastal water transition zone during the initial period, 1960-1964, of the dramatic Aral Sea changes.

Methodology and flow model

We model a representative cross-section of the south-eastern part of the Large Aral Sea groundwater-coastal water transition zone, where the Amu Darya delta is situated (see Figure 1), using the U.S. Geological Survey SUTRA code (Voss, 1984) that can handle density-dependent flows. Figure 2 shows the modeled cross-section, and its initial hydrostatic boundary conditions and salinity distribution. No-flow is specified at the bottom of the aquifer and at the top of the land surface, assuming that the net groundwater recharge is negligible due to the arid climate in the Aral Sea region. Fresh water inflow is given by specifying a constant hydrostatic pressure along the landside boundary, assuming that the groundwater table is located on average 3m below surface at this boundary. We use this constant head boundary, rather than a constant flow boundary, because it is consistent with the relatively constant annual average groundwater levels that characterize the (surrounding) irrigated fields. Hydrostatic seawater pressure is initially imposed along the seaside boundaries A and B, where a transient boundary condition is to be imposed at a later stage to simulate the decreasing Aral Sea level. Regarding salt concentrations, the salinity level (TDS) of freshwater initial conditions and inflow into the aquifer is assumed to be 0.5 g/L. Along the seaside boundaries A and B, the corresponding seawater salinity level is specified to be 10 g/L, in agreement with the Aral Sea salinity of 1960.

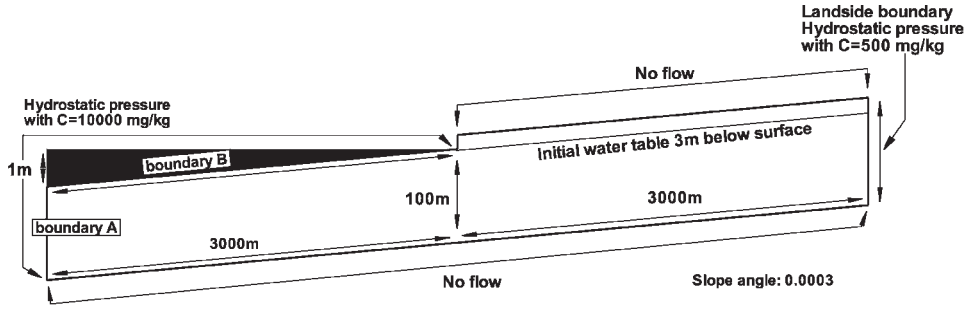

Figure 2. Schematic illustration of the simulated aquifer cross-section, representative of the South–Eastern Aral Sea coast in 1960.

Before proceeding to the transient simulation of the Aral Sea shoreline recession, the initial groundwater flow and salt content conditions are obtained by long–term transient simulations until reaching steady-state conditions, with equal and temporally unchanging flows into and from the system. Table 1 lists physical and numerical values used in the SUTRA simulations, which remain the same during the simulations except for the seawater density. We then simulate the groundwater dynamics caused by the receding Aral Sea shoreline and associated increasing salt content over the considered simulation period 1960-1964 using transient boundary conditions. Along the seaside boundaries A and B, hydrostatic pressure decreases with time, according to observed sea level changes (Mamatov, pers. com.). The increasing salinity values were accounted for through linear regression analysis of the observed salinity values (Mamatov, pers. com.) between 1960 and 1969. Hence, while water pressure at the upper sea sediment boundary reduces with receding shoreline, the resulting increased seawater salinity yields a pressure increase due to increased seawater density. The new land surface that appears as the shoreline recedes is excluded from the sea boundary B during the simulation. The shoreline displacement observed during the presently considered simulation time-period 1960-1964 is still ongoing as is the salinisation of the Aral Sea water, which will be addressed in following work.

Table 1. Physical and numerical parameter values used in the simulations.

Parameter	**Value**
Representative width of simulated cross-section (m)	6000
Formation depth (m)	103
Number of elements	3134
Number of nodes	2880
Spatial discretisation	
Horizontal, Δx (m)	25
Vertical 1: Δy_1 (m)	9.99[a]
Vertical 2: Δy_2 (m)	0.01[b]
Vertical 3: Δy_3 (m)	1.5[c]
Mean effective natural groundwater recharge N_R ($m^3 year^{-1} m^{-1}$)	0
Mean saturated hydraulic conductivity (ms^{-1})	$3.0 \cdot 10^{-5}$
Effective porosity	0.36
Longitudinal dispersivity (m)	6.25
Transverse dispersivity (m)	1.0
Fluid compressibility	0
Fluid viscosity ($kg\ m^{-1} s^{-1}$)	10^{-3}
Aquifer matrix compressibility	0
Parameter a in Van Genuchten equation ($m\ s^2\ kg^{-1}$)	$5 \cdot 10^{-5}$
Parameter b in Van Genuchten equation	2
Residual degree of saturation	0.3
Molecular diffusivity ($m^2\ s^{-1}$)	10^{-9}
Base solute concentration ($mg\ kg^{-1}$)	500
Freshwater density ($kg\ m^{-3}$)	999.73
Initial seawater density ($kg\ m^{-3}$)	1007.5
Density change with concentration coefficient ($kg^2\ conc.^{-1} m^{-3}$)	700

[a]For elements below the uppermost soil layer of 3.01 m and below the seabed layer of 0.01m.
[b]For elements within the uppermost seabed layer of 0.01m, and between 3.01 and 3m below the uppermost soil layer.
[c]For elements within the uppermost soil layer of 3 m.

Results

Figures 3a and 3b show the resulting flow development over the simulation period 1960-1964 for the seaside boundary A, QA, and boundary B, with QB being the net flow and QSGD only the discharge into the sea at that boundary, the upstream landside boundary, QFWI, and the net sum of flows through all system boundaries, QNET (see Figure 3c for an illustration of the different flow components). Flow components in Figure 3a indicate recharge (i.e. inflow) into the system whereas flow components in Figure 3b indicate discharge (i.e. outflow) from the system. For comparison, the observed sea level decrease is also shown in Figures 3a and 3b (data from Mamatov, pers. comm.). The SGD boundary B, QSGD, includes the discharge and QB the net flow into the sea of mixed seawater and freshwater components through

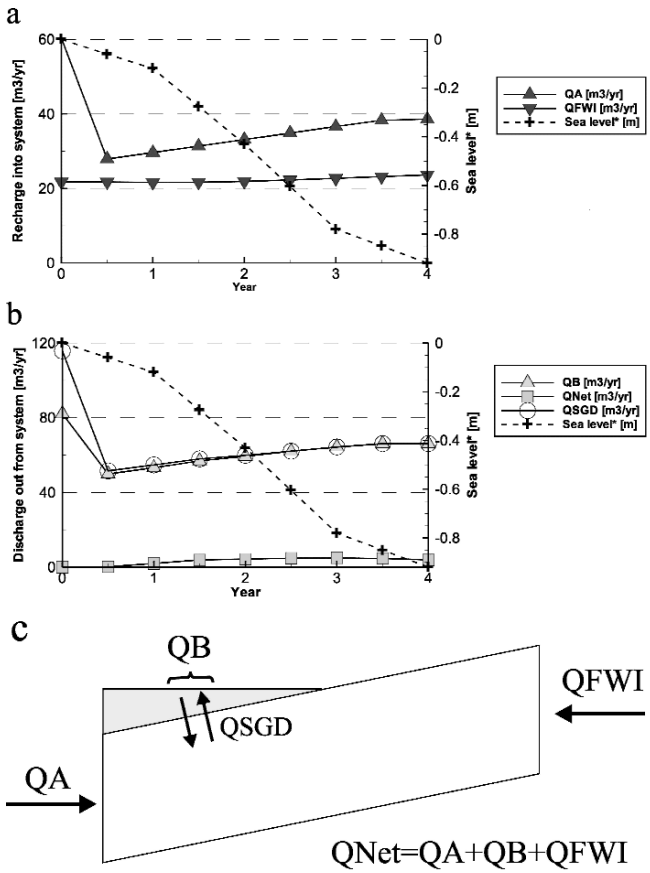

Figure 3. Resulting flow development over the simulation period 1960-1964 for: (a) the seaside boundary A, QA, and the upstream landside boundary, QFWI; and (b) the seaside boundary B, with QB being net flow and QSGD only the discharge into the sea at that boundary, and the net sum of flows through all system boundaries, QNET. Flow components in (a) indicate recharge (i.e., inflow) into the system whereas components in (b) indicate discharge (i.e., outflow) out from the system. For comparison, the associated observed sea level decrease is also shown (data from Mamatov, pers. comm.). Figure (c) illustrates schematically the different components.

boundary B. The figures show that, apart from an initial period, there is essentially only discharge into the sea through the seaside boundary B, while recharge occurs through the landside boundary and the seaside boundary A. Furthermore, the pure discharge component QSGD exhibits an initial decrease followed by small yet steady increase, and the freshwater flow QFWI increases throughout the transient simulation.

The generally quite small flow changes over the simulation period, during which the sea level and shoreline change quite considerably, are explained by the fact that the regional hydraulic gradient is forced to remain approximately the same by the flat coastal topography and bathymetry of this region (see further Jarsjö and Destouni, 2004). Furthermore, the seawater salinity and associated density changes are relatively small within the simulated time period.

Figure 4 further shows the salinity transition zone and associated streamlines for the initial dynamic equilibrium condition, and after the 4 years of transient simulation. The streamlines in Figures 4a and b originate from the same fixed positions at the landside boundary, which are located outside of Figure 4, but can be seen in Figure 5. Initially, the simulated salinity transition zone extends approximately one kilometer inland from the original shoreline (Figure 4a). Due to density differences, the main freshwater discharge into the Aral Sea then occurs in the nearest vicinity of the original shore, as shown by the streamlines in Figure 4a. The continuous sea level decrease and associated shoreline recession of 2.8 kilometres (outside of the cross-section shown in Figure 4b, but shown in Figure 5) do not significantly change the position of the salinity transition zone during the simulation period due to the very low simulated groundwater velocity, approximately 0.7 m/year on average. This movement, however, does stop the recharge and following discharge of re-circulating seawater through boundary B, in the vicinity of the original shoreline position (compare seawater streamlines in Figures 4a and 4b), while the seaward fresh groundwater discharge increases (see QFWI in Figure 3a) and flows through the sediments under the sea, rather than as SGD into the sea, at the original shoreline position (see streamlines in Figure 4b). Since the movement of groundwater is generally very slow in this model, the transition zone will require very long time to reach its new dynamic equilibrium condition with a new (stabilized) shoreline at a lower elevation. This means that the transition zone will exist in the vicinity of its initial location for very long time periods.

Figure 5 illustrates the changing flow patterns over the whole considered cross sections, in contrast to the close-ups of Figure 4. Hence, Figure 5a shows the whole flow field for the salinity distribution illustrated in Figure 4a, and Figure 5c shows the whole flow field for the salinity distribution illustrated in Figure 4b. A comparison between Figures 5a and 5b shows that the recharge and discharge of re-circulating seawater through boundary B (in the vicinity of the original shoreline position) essentially stops soon after the sea level starts to decrease (in the beginning of the simulation period). This lack of recirculation explains the initial decrease in QSGD shown in Figure 3b and the fact that the net flow QB through the same seaside boundary B equals QSGD afterwards. The initially intruded seawater, which lost supporting hydrostatic seawater pressure due to the receded shore, is now under a non-equilibrium condition and therefore starts to flow towards sea, appearing as a steady increase in QSGD after the initial drop, seen in Figure 3b. The flow pattern to the very left in Figure 5 (around x=-3000m) was found to change in response to relatively small changes in assumed conditions at boundaries A and B, however, this artifact did not influence the flow pattern in rest of the domain (i.e., $x > \sim -2800$). Furthermore, the streamline development over time that is illustrated by Figures 5a-c shows that fresh groundwater discharge after the start of the continuous sea-level decrease continues to flow through the sediments at the original salinity

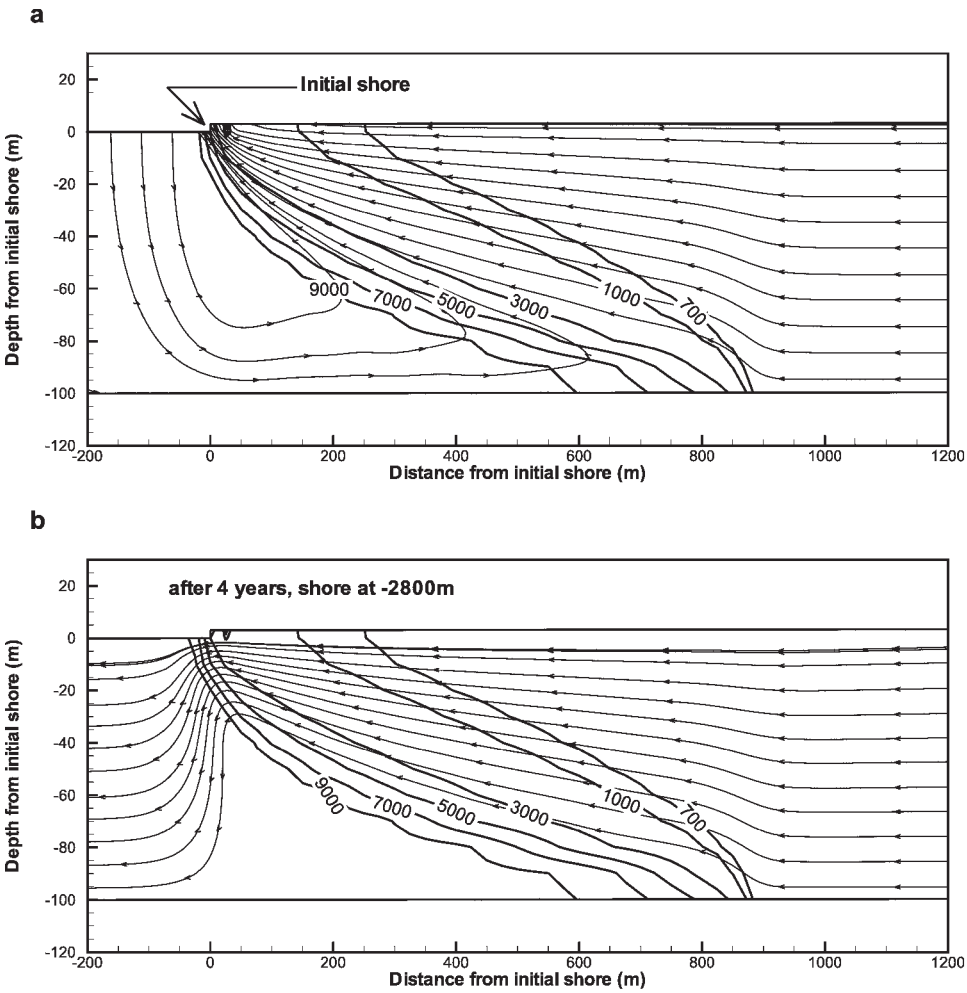

Figure 4. Resulting salinity transition zone (isolines with units mg·kg^{-1}) and streamlines (a) originally, before the shore recession, and (b) after 4 years of simulated continuous sea level decrease and shoreline recession.

transition zone and shoreline location (instead of into the sea as SGD; Figure 5a), where it will gain salinity and density through mixing with seawater and continue to flow essentially horizontally towards the new shoreline position. If the shoreline continues to move due to continued sea-level decrease, the groundwater will also continue to flow essentially horizontally through the sediments until the shoreline stabilizes at some location, where groundwater is forced to flow up into the sea as SGD by the still higher density of pure seawater.

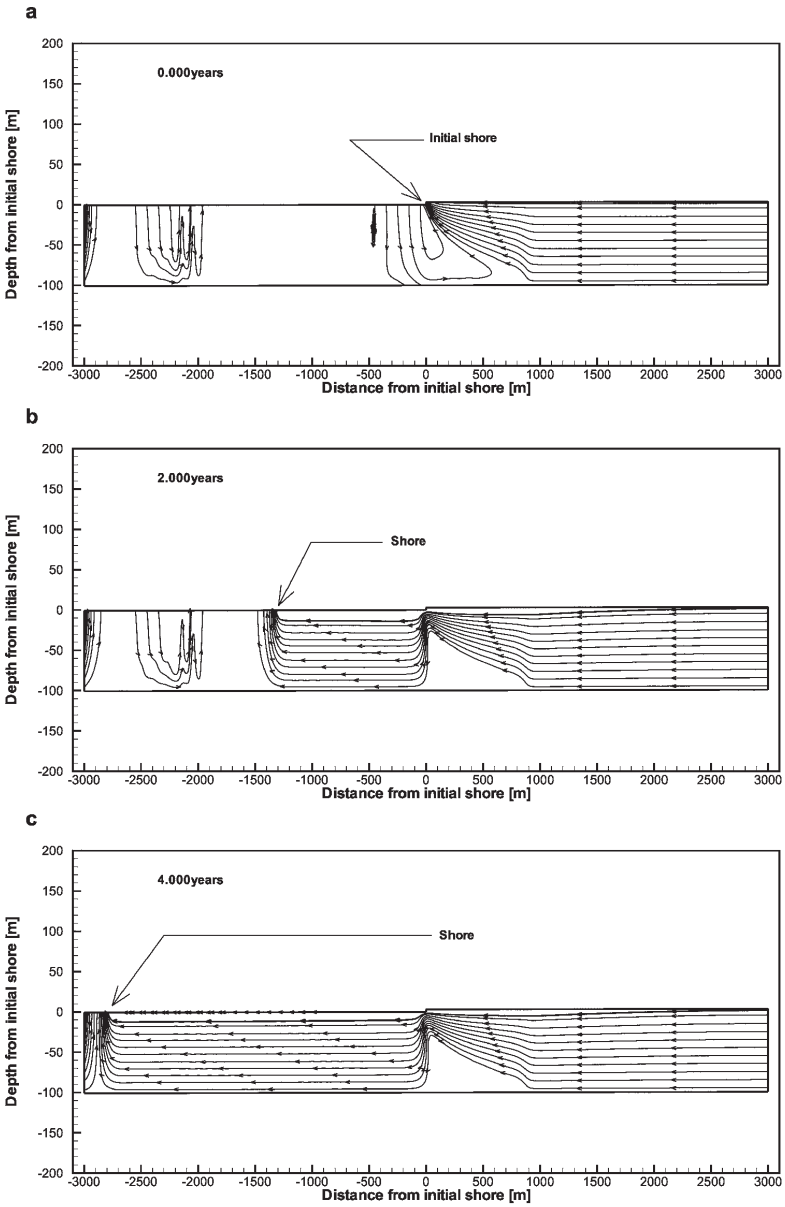

Figure 5. Resulting streamlines: (a) at initial conditions, (b) after 2 years of simulation, and (c) after 4 years of simulation.

Conclusions

Considering the Aral Sea surface level lowering and the associated seaward shoreline movement of 2.8 kilometres and seawater salinity change during the period 1960-1964, our results indicate that the net

SGD into the Aral Sea exhibited an overall decrease over this period, although there is a trend of increase following the relatively large initial decrease. The seaward fresh groundwater discharge exhibits a small yet systematic increase over the simulation period, during which seawater density did not change much and the mean groundwater hydraulic gradient could not change much, due to the generally flat coastal topography and bathymetry of the South-Eastern Aral Sea coast. Groundwater in the vicinity of the original, pre-1960 shoreline, remained brackish, with salinity around 10 g/L, indicating a remaining aquifer vulnerability to seawater intrusion.

Acknowledgements

Financial support for this work was provided by SIDA (the Swedish International Development Cooperation Agency) and the EU INTAS Aral Sea Call 2000, project number 1014.

References

ALADIN, N.V., PLOTNIKOV, I.S. and LETOLLE, R., (2004). Hydrobiology of the Aral Sea. In: NIHOUL, J.C.J., ZAVIALOV, P.O., and MICKLIN, P.P. (Eds.), *Dying and Dead Seas: Climatic Versus Anthropic Causes*. NATO science series, Kluwer Academic Publishers, Dordrecht, The Netherlands, 125-157.

FROEBRICH, J. and KAYUMOV, O., (2004). Water Management Aspects of Amu Darya. Options for future strategies. In: NIHOUL, J.C.J., ZAVIALOV, P.O. and MICKLIN, P.P. (Eds.), *Dying and Dead Seas: Climatic Versus Anthropic Causes*. NATO science series, Kluwer Academic Publishers, Dordrecht, The Netherlands, 49-76.

JARSJÖ, J. and DESTOUNI, G., (2004). Groundwater discharge into the Aral Sea after 1960. *Journal of Marine Systems*, 47, 109-120.

KOSTIANOY, A.G., ZAVIALOV, P.O. and LEBEDEV, S.A., (2004). What do we know about dead, dying and endangered lakes and seas. In: NIHOUL, J.C.J., ZAVIALOV, P.O. and MICKLIN, P.P. (Eds.), *Dying and Dead Seas: Climatic Versus Anthropic Causes*. NATO science series, Kluwer Academic Publishers, Dordrecht, The Netherlands, 1-48.

KOUSSIS, A.D., KOTRONAROU, A., DESTOUNI, G. and PRIETO, C., (2002). Intensive groundwater development in coastal zones and small islands. In: LLAMAS, R. and CUSTODIO, E. (Eds.), *Groundwater Intensive Use: Challenges and Opportunities*. ISBN: 90 5809 390 5, Balkema, The Netherlands, 133-155.

MAMATOV, S., Personal communication based on data from the State Committee for Hydrometerology of the Republic of Uzbekistan and Institute of Bioecology of Science Academy of the Republic of Uzbekistan.

MOORE, W.S., (1996). Large groundwater inputs to coastal waters revealed by ^{226}Ra enrichments. *Nature*, 380, 612-615.

VOSS, C.I., (1984). Saturated – Unsaturated TRAnsport. U.S. Geological Survey Water-Resources Investigations Report 84-4369, USGS.

ZAVIALOV, P.O., KOSTIANOY, A.G., EMELIANOV, S.V., NI, A.A., ISHNIYAZOV, D., KHAN, V.M. and KUDYSHKIN, T.V., (2003). Hydrographic survey in the dying Aral Sea. *Geophysical Research Letters* 30 (13), 1659 (doi:10.1029/2003GL017427).